Reversible diameter modulation of single-walled carbon nanotubes by acetonitrile-containing feedstock

Theerapol Thurakitseree,[†] Christian Kramberger,[‡] Shohei Chiashi,[†]

Erik Einarsson,[†,¶] and Shigeo Maruyama[*,†]

Department of Mechanical Engineering, The University of Tokyo, 7-3-1 Hongo, Bunkyo-ku, Tokyo 113-8656, Japan, Faculty of Physics, University of Vienna, Strudlhofgasse 4, Vienna, A-1090, Austria, and Global Center of Excellence for Mechanical Systems Innovation, The University of Tokyo, 7-3-1 Hongo, Bunkyo-ku, Tokyo 113-8656, Japan

E-mail: maruyama@photon.t.u-tokyo.ac.jp

Phone: +81 (0)3 5841 6421. Fax: +81 (0)3 5800 6983

Abstract

Changing the carbon feedstock from pure ethanol to a 5 vol.% mixture of acetonitrile in ethanol during the growth of vertically aligned single-walled carbon nanotubes (SWNTs) reduces the mean diameter of the emerging SWNTs from 2 to 1 nm. This feedstock-dependent change is found to be independent of supply sequence, as demonstrated by triple-layer vertically aligned SWNT structures. The reversibility of this process indicates it is catalyst independent, and opens up new possibilities in bottom-up engineering of SWNT-based devices.

[*]To whom correspondence should be addressed

[†]Department of Mechanical Engineering, The University of Tokyo, 7-3-1 Hongo, Bunkyo-ku, Tokyo 113-8656, Japan

[‡]Faculty of Physics, University of Vienna, Strudlhofgasse 4, Vienna, A-1090, Austria

[¶]Global Center of Excellence for Mechanical Systems Innovation, The University of Tokyo, 7-3-1 Hongo, Bunkyo-ku, Tokyo 113-8656, Japan

Introduction

The properties of single-walled carbon nanotubes (SWNTs) are strongly dependent on their structure and become more enhanced as the nanotube diameter decreases. As a result, chirality and diameter control—particularly during synthesis—offers great potential for tuning the SWNT properties. It is widely accepted that the SWNT diameter is largely determined by the size of the catalyst nanoparticle, and this size relationship has been thoroughly studied.[1–10] Fiawoo et al.[8] recently reported an analogue of catalyst particle size and SWNT diameter, and found that SWNTs directly grown by chemical vapor deposition (CVD) can resemble the catalyst particle size when the growth condition is close to thermodynamic equilibrium. A gradual increase of mean diameter with increasing growth temperature[11–13] as well as during the growth process of vertically aligned SWNTs (VA-SWNTs)[10,14] has also been observed. Chirality changes at intramolecular junctions due to temperature increase have been observed earlier in individual SWNTs[11] and double-walled CNTs (DWNTs).[13] These intramolecular junctions were identified as a continuous sp^2 network with local lattice distortions.[12] Structural changes via other parameters such as feedstock have not yet been explored.

In this study, we demonstrate reversible diameter modulation of VA-SWNTs by switching between pure ethanol and nitrogen-containing precursors during synthesis. VA-SWNTs were synthesized by no-flow CVD from cobalt/molybdenum (Co/Mo) binary catalysts.[15–17] Based on spectroscopic analysis, the mean SWNT diameter was found to change between 2.1 nm when using pure ethanol, to less than 1 nm for a feedstock containing 5 volume percent (5 vol.%) acetonitrile in ethanol.[18–20] This change was observed regardless of the sequence in which the carbon feedstocks were introduced.

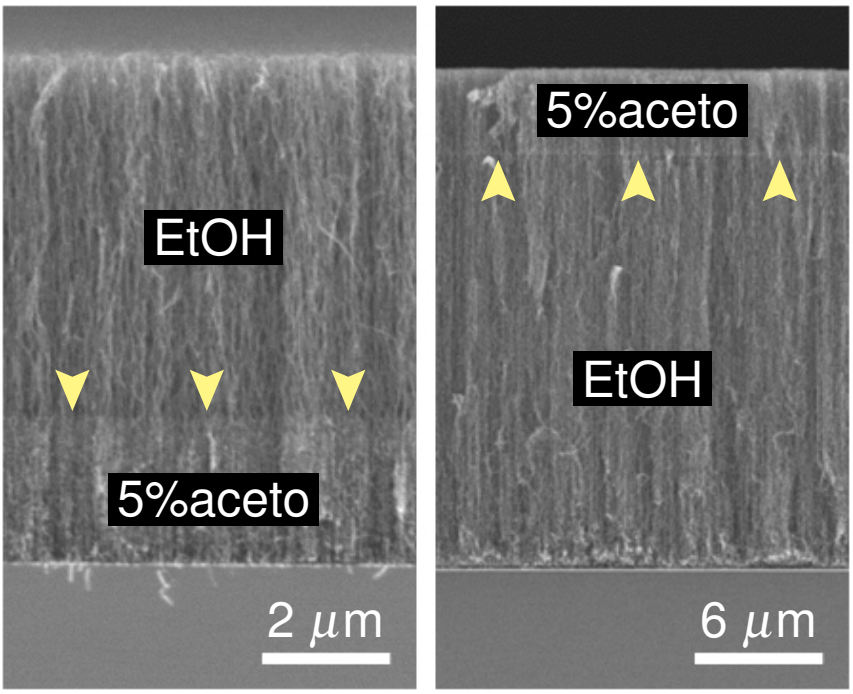

Figure 1: SEM images of double-layer VA-SWNT arrays synthesized from ethanol (EtOH) and 5 vol.% acetonitrile (5%aceto). Left and right panels show different feedstock sequence, with growth initiated by EtOH (left) and 5%aceto (right). Yellow arrows mark the interface between the regions grown from different feedstocks.

Results and Discussion

Catalyst-Independent Diameter Modulation

Figure 1 demonstrates double-layer growth of SWNTs. The left panel shows VA-SWNTs in which the feedstock was changed from ethanol (EtOH) to 5 vol.% acetonitrile (5%aceto). The right panel shows VA-SWNTs grown from the reversed sequence of carbon feedstocks. Since the formation of VA-SWNTs is known to be a root-growth process,[17] the top part of the array is formed first and the part nearest the substrate is formed last. The interface between the EtOH-grown and 5%aceto-grown regions is clearly visible in the SEM images (indicated by arrows in Fig. 1).

Figure 2 shows growth profiles of the VA-SWNT arrays shown in Fig. 1. The growth process was monitored in real-time using *in situ* optical absorbance.[16,21] The two stages are depicted by blue and red lines for EtOH and 5%aceto, and the initial growth rates of SWNTs synthesized from EtOH (*Et*-SWNT) and 5%aceto (*Ac*-SWNT) are 3 and 1.5 μm per minute, respectively. The

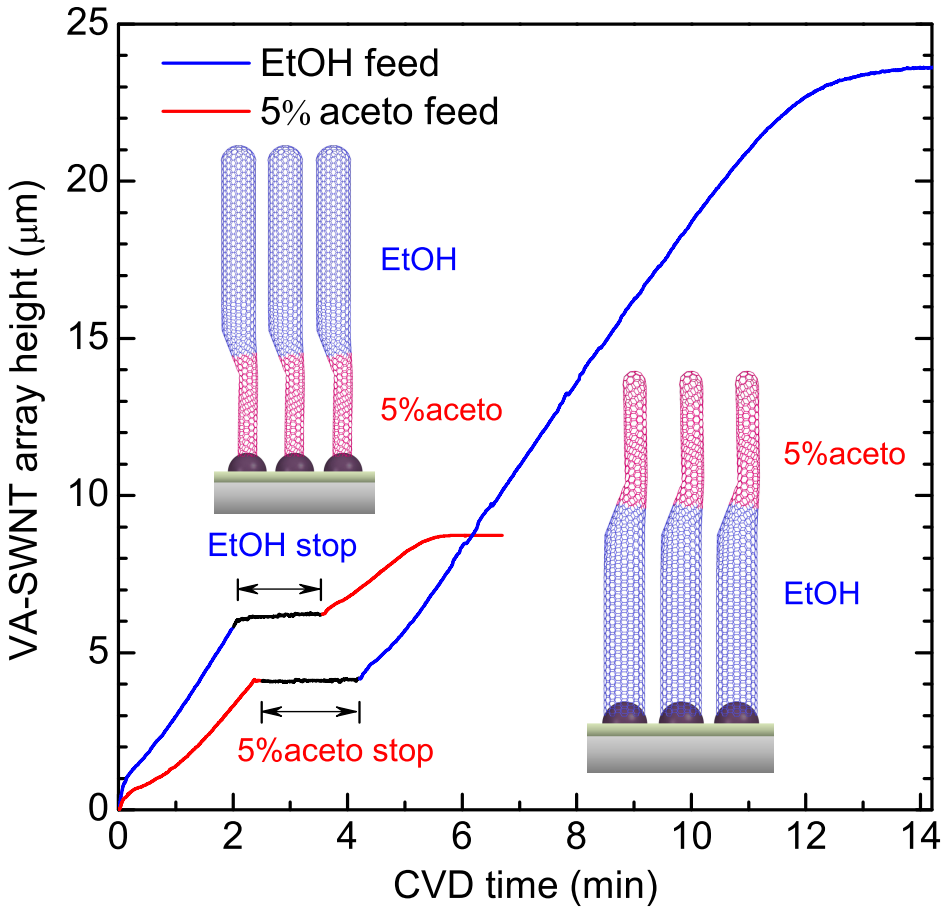

Figure 2: Growth curves of double-layers SWNT arrays synthesized from ethanol (EtOH) and 5%acetonitrile (5%aceto) monitored by *in-situ* measurement. Blue and red labels represent SWNTs synthesized from EtOH and 5%aceto feedstocks, respectively.

different growth rates indicate an influence of N-containing species on the reaction dynamics.[22]

Figure 3 shows resonance Raman spectra of double-layer VA-SWNTs obtained using an excitation wavelength of 488 nm from cleaved side walls. The radial breathing mode (RBM) peaks reveal specific SWNTs that are in resonance with the 488 nm laser, and the frequency is diameter dependent.[23,24] Here we used the empirical relation[25] $\omega_{\mathrm{RBM}} = 217.8/d + 15.7$ to estimate the tube diameter, where ω_{RBM} is the Raman shift in cm^{-1} and d is the tube diameter in nm. The very different Raman spectra obtained from as-grown *Et*-SWNT and *Ac*-SWNT are shown in Figure 3a. The increased D-line intensity is a common characteristic once N is incorporated.[26,27] In the case of *Ac*-SWNT, the 488 nm excitation wavelength is in resonance with the first optical transition of small-diameter metallic SWNTs $\left(E_{11}^{M}\right)$, as seen in the appearance of the RBM peaks at 240 and

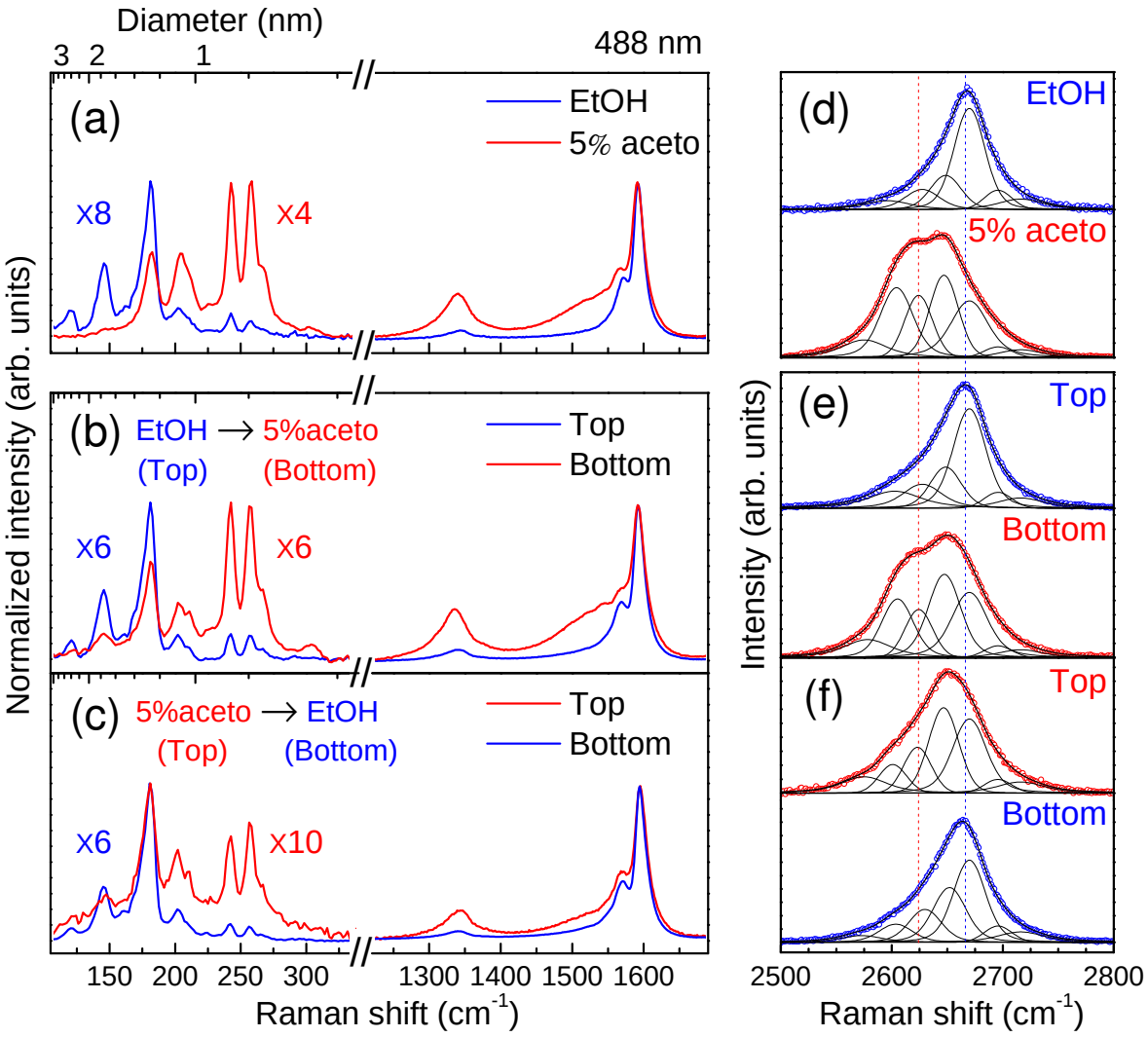

Figure 3: Resonance Raman spectra for RBM and G band (a-c) and the 2D (G′) peak region (d-f) of different SWNT layers synthesized from ethanol (EtOH, blue line/label) and 5 vol.% acetonitrile (5%aceto, red line/label) feedstocks. Excitation wavelength is 488 nm and the laser is polarized perpendicular to the nanotube axis.

260 cm^{-1} and increasing intensity of the Breit-Wigner-Fano (BWF) line shape. Peaks from larger-diameter semiconducting *Et*-SWNT at 145 and 160 cm^{-1} originate from resonances of the third $\left(E_{33}^{S}\right)$ and fourth $\left(E_{44}^{S}\right)$ optical transitions.

Figure 3 reveals catalyst-independent change in the diameter of SWNTs when changing the feedstock gas from EtOH to 5%aceto (*Et*→*Ac*-SWNT), as well as the reverse (*Ac*→*Et*-SWNT). Spectra from VA-SWNTs synthesized from an unchanging feedstock gas (*Et*-SWNT or *Ac*-SWNT) are shown for reference (Figs. 3a and 3d). The strong BWF feature and D-line of the 5%aceto layer

are identical to the features found in the *Ac*-SWNT spectrum (Fig. 3a). The diameter along the array is reduced in *Et*→*Ac*-SWNT when the feedstock is switched to 5%aceto, as seen in Fig. 3b by the dominant appearance of small-diameter RBM peaks around 230-270 cm^{-1} ($d < 1$ nm).[18] On the other hand, in *Ac*→*Et*-SWNT an increase in diameter (up to 2.1 nm) is observed (Fig. 3c) with RBM peaks appearing between 140 and 220 cm^{-1} when EtOH is introduced later. The interface between the two arrays is clearly observed as the diameter changes significantly.

Resonance Raman spectra of the 2D (G′) line were obtained using the same 488 nm excitation wavelength (Fig. 3(d-f)). Blue and red open circles represent the G′ spectra of VA-SWNTs synthesized from EtOH and 5%aceto, respectively. The G′ peaks were decomposed using two Voigtian peaks at 2620 and 2666 cm^{-1} for *Et*-SWNT, *Et*→*Ac*-SWNT (top layer) and *Ac*→*Et*-SWNT (bottom layer), and three Voigtian peaks at 2610, 2650 and 2680 cm^{-1} for *Ac*-SWNT, *Et*→*Ac*-SWNT (bottom layer) and *Ac*→*Et*-SWNT (top layer). All peak components (black solid lines) were fitted with a constant full-width at half-maximum (FWHM) of 19.7 cm^{-1}.

Figures 3(d-f) show identical G′ spectra of EtOH-grown SWNT arrays at the position of 2666 cm^{-1} in all cases. The similar spectra of 5%aceto-grown SWNTs were obtained from *Ac*-SWNT, *Et*→*Ac*-SWNT (bottom layer) and *Ac*→*Et*-SWNT (top layer). A large downshift is due to the vast difference in SWNT diameter, which has been observed in previous studies on N-doped SWNTs.[18,28,29] These data clearly show that *Ac*-SWNTs and *Et*-SWNTs always have their characteristic diameter distribution, regardless of the sequence of feedstock introduction.

Reversible Diameter Change

In order to investigate the reversibility of this process, triple-layer growth was performed by first introducing 5%aceto, followed by EtOH, and again 5%aceto. A cross-sectional SEM image of the resulting VA-SWNT array is shown in Fig. 4a. Arrows are again used to mark the clear interfaces where the precursor was changed. Resonance Raman spectra (488 nm excitation wavelength) were obtained along the height of the array at the corresponding positions indicated by points 1 to 7 in Fig. 4a. The Raman spectra obtained at these points are shown in Fig. 4b. The very sharp and

reversible change to smaller diameters ($d < 1$ nm) as well as the metallic BWF feature in the G-line clearly identify the 5%aceto-grown layers at the top and the bottom of the sandwich structure (red points 1, 2, 6, and 7). The characteristic Raman features of VA-SWNTs synthesized from EtOH[15] are, in contrast, observed in the central layer (blue points 3 to 5). RBM peaks at 203, 242 and 257 cm^{-1} corresponding to small-diameter SWNTs significantly decrease in intensity when the laser focus dwells on the central layer.

Several methods to alter the SWNT structure during growth have been demonstrated by changing growth temperature,[1,9] and/or pressure.[30,31] The catalyst particle size certainly restricts the largest possible SWNT diameter, but smaller SWNTs rooting from larger catalyst particles are entirely conceivable. The change in diameter along the nanotube axis as temperature decreases has been previously reported in individual SWNTs,[11] DWNTs,[13] and other configurations of intramolecular junctions.[32–37] In previous studies,[11,13] it was reported that small-diameter nanotubes preferentially grow when the temperature is increased from 900°C to 950°C, which may be explained by an altered shape of the catalyst particles. These scenarios are, however, catalyst-dependent growth. Changes in chirality and diameter may be achieved by introducing defects in the hexagonal lattice.[12,38,39] It is also well-established that incorporation of nitrogen will easily induce defects into the SWNT structure.[40] Hence, the possibility of chirality change due to the presence of nitrogen during synthesis is a viable scenario.

Since the diameter is reversible, we consider two possible growth mechanisms: (1) SWNTs with different diameters can grow from the same catalyst nanoparticle, and (2) catalyst particles of different size are active under different feedstock conditions.

The presence of N has to be considered to see how a catalyst particle can be caused to favor an SWNT with much smaller diameter. Density functional theory (DFT) calculations have shown that Co-N has a higher binding energy (*i.e.* stronger adhesion) than Co-C.[41] The impeded growth rate in the presence of N may therefore be related to a stronger adhesion between the sp^2 network and the catalyst particle. This condition has been predicted to result in narrower SWNTs.[42] If the growth takes place from the same catalyst particle, then the relatively moderate changes in

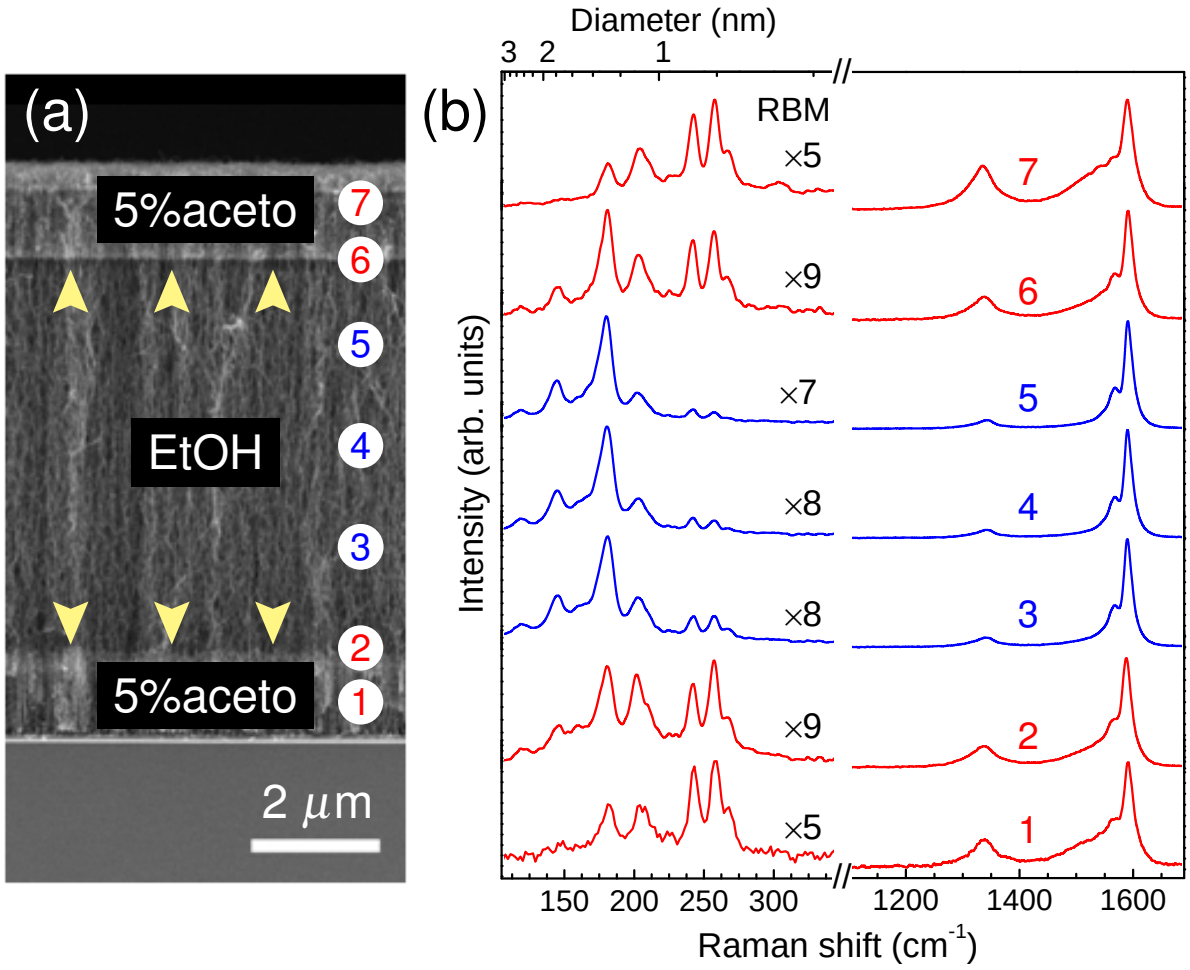

Figure 4: Reversibility of SWNT diameter demonstrated by three layer growth of SWNT arrays characterized by SEM image (a) and 488 nm resonance Raman spectra (b). The yellow arrows denote the interfaces between different SWNT layers. The laser is polarized perpendicular to the nanotube axis.

feedstock first cause a narrow SWNT to nucleate and grow from larger catalyst particles, with the SWNT diameter being independent of catalyst size. The effect of 5 vol.% acetonitrile in the feedstock is to maintain the narrow diameter. Once the acetonitrile is gone, the narrow tube relaxes by incorporating defects, and the same tube continues to grow with a larger diameter. If acetonitrile is re-introduced the SWNT growth conditions again favor smaller diameters. This scenario is shown in Fig. 5(a).

Another possible mechanism is discontinuous growth (Fig. 5(b)). SWNT growth from different catalyst particles would require selective and reversible activation and deactivation of catalyst par-

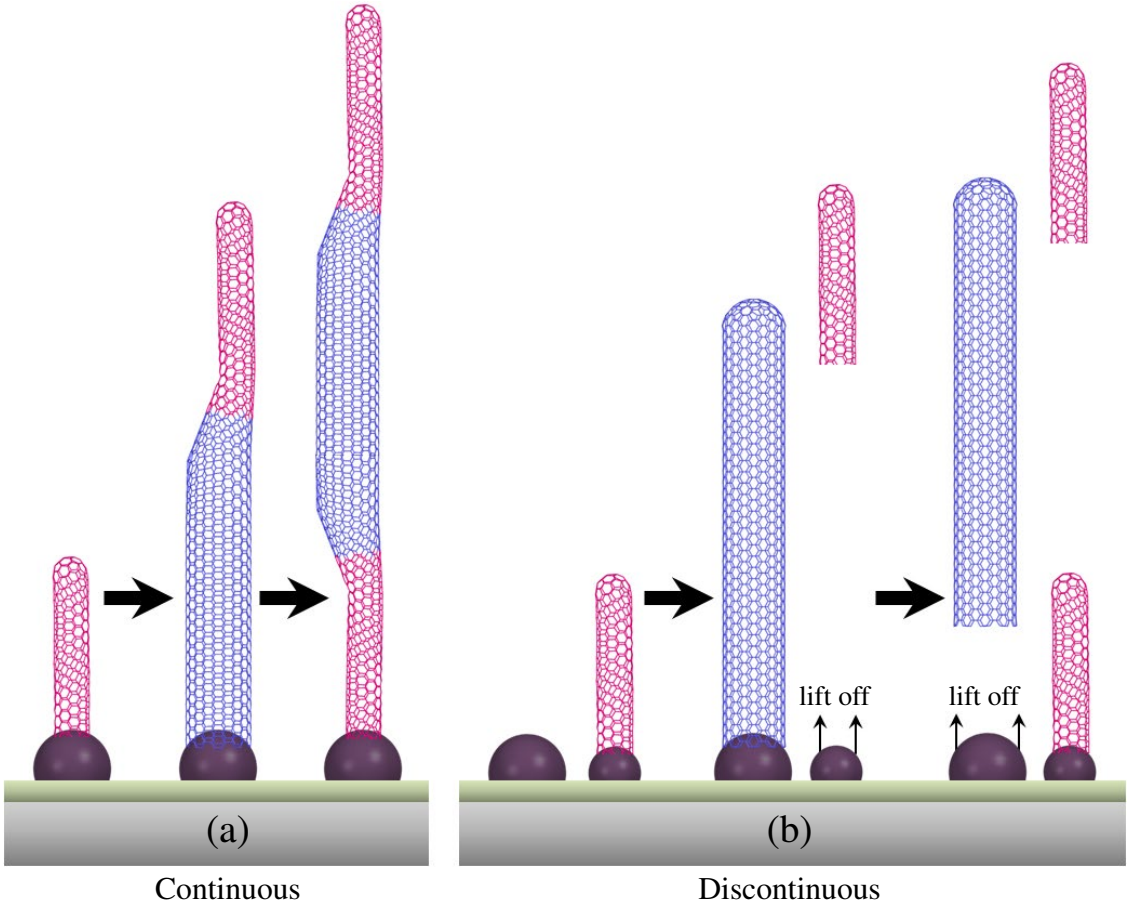

Figure 5: A possible mechanism of three layer growth of different diameter VA-SWNTs from Co catalyst nanoparticles. Blue and red tubes represent SWNTs synthesized from ethanol (EtOH) and 5 vol.% acetonitrile (5%aceto), respectively.

ticles with a variety of sizes every time the feedstock is changed. Small-diameter SWNTs would grow in the presence of acetonitrile while larger catalyst particles lie dormant. When acetonitrile is absent, the small catalyst particles would stop growing SWNTs and the larger particles would become active. In this case, the adhesion forces among the VA-SWNTs must be strong enough that the driving force of subsequent growth from different catalyst particles could detach and push up the layer of previously grown SWNTs. The same detachment and uplift would then need to take place again when the feedstock is switched back.

Considering these two possible explanations for the changing diameter, we conclude that the former case—in which diameter changes along continuously growing SWNTs—is the more likely scenario. While both of the above scenarios are equally capable of explaining the single layer

growth of either ethanol VA-SWNTs or 5%aceto VA-SWNTs, the double and especially triple layer growth start to become more and more unlikely with growth from different particles, especially when considering that the ethanol concentration only changes by 5%. Therefore, the sandwiched triple layer convincingly demonstrates that changes in the feedstock composition can change the diameters of growing SWNTs *on-the-fly*, and growth is likely from the same catalyst particles.

Conclusion

We demonstrate multi-layered growth of vertically aligned SWNTs in which the layers have vastly different diameters. Our empirical finding of reversible diameter change suggests that the diameter of VA-SWNTs can be controlled solely by changing the feedstock. The mean diameter of each layer is controlled by the choice of feedstock, and changes from 2.1 nm when using pure ethanol to less than 1.0 nm when using 5 vol.% acetonitrile in ethanol. The different layers are distinguishable by SEM, and resonance micro-Raman spectroscopy clearly reveals the significant diameter change. Synthesis of a triple-layer structure shows the diameter changes are consistent and reversible, thus is most likely explained by diameter change along continuous SWNTs rather than growth termination and re-nucleation from different catalyst particles. The ability to easily and efficiently modulate the nanotube diameter during SWNT growth is crucial for bottom-up fabrication of carbon nanotube materials and devices.

Methods

No-flow CVD was employed for synthesis of VA-SWNTs.[17] The Co/Mo binary catalysts were prepared as in our previous report.[15] Pure ethanol (EtOH) and a mixture of 5 vol.% of acetonitrile in ethanol (5%aceto) were used as precursor. Catalysts deposited on quartz or silicon substrates were reduced by flowing 300 sccm of Ar/H_2 (3% H_2) during heating (approximately 30 min). After reaching 800°C, the CVD chamber was evacuated and 40 μL of a liquid precursor was introduced by opening a valve. EtOH was first introduced into the reaction chamber for 2 min, after which the

CVD chamber was evacuated prior to introducing 5%aceto until the growth stopped. The CVD chamber was then cooled under flowing Ar. This growth is hereafter referred to as *Et*→*Ac*-SWNT. If the feedstocks were introduced in the reverse order, the growth is referred to as *Ac*→*Et*-SWNT. The growth of VA-SWNTs was monitored *in-situ* by a calibrated real-time measurement of the attenuation of a He/Ne (633 nm) laser passing through a quartz substrate supporting the growing films.[21] VA-SWNT arrays synthesized from only EtOH or only 5%aceto are referred to as *Et*-SWNT and *Ac*-SWNT, respectively.

The morphology of the resulting multi-layered VA-SWNT arrays was imaged by scanning electron spectroscopy (SEM, 1 kV acceleration voltage, S-4800, Hitachi Co., Ltd.). For resonance Raman spectroscopy (Chromex 501is with Andor DV401-FI), a laser with excitation wavelength of 488 nm was incident on the cleaved cross-section of the VA-SWNT films using a 50× objective lens with a laser power of 0.5 mW. For cross-sectional Raman measurement in Fig. 3 and Fig. 4, the incident laser was polarized perpendicular to the nanotube axis in order to observe clearer differences between *Et*-SWNT and *Ac*-SWNT.[43]

Acknowledgement

Part of this work was financially supported by Grants-in-Aid for Scientific Research (22226006, 23760180 and 23760179), JSPS Core-to-Core Program, and the Global COE Program "Global Center for Excellence for Mechanical Systems Innovation". TT acknowledges support from the Higher Educational Strategic Scholarships for Frontier Research Network (CHE-PhD-SFR) granted by the Office of Higher Education Commission, Thailand. CK acknowledges the Austrian Academy of Sciences for the APART fellowship A-11456.

References

1. Bandow, S.; Asaka, S.; Saito, Y.; Rao, A. M.; Grigorian, L.; Richter, E.; Eklund, P. C. Effect of the Growth Temperature on the Diameter Distribution and Chirality of Single-Wall Carbon Nanotubes. *Phys. Rev. Lett.* **1998**, *80*, 3779–3782.

2. Kataura, H.; Kumazawa, Y.; Maniwa, Y.; Ohtsuka, Y.; Sen, R.; Suzuki, S.; Achiba, Y. Diameter Control of Single-Walled Carbon Nanotubes. *Carbon* **2000**, *38*, 1691–1697.

3. Kitiyanan, B.; Alvarez, W. E.; Harwell, J. H.; Resasco, D. E. Controlled Production of Single-Wall Carbon Nanotubes by Catalytic Decomposition of CO on Bimetallic Co-Mo Catalysts. *Chem. Phys. Lett.* **2000**, *317*, 497–503.

4. An, L.; Owens, J. M.; McNeil, L. E.; Liu, J. Synthesis of Nearly Uniform Single-Walled Carbon Nanotubes using Identical Metal-Containing Molecular Nanoclusters as Catalysts. *J. Am. Chem. Soc.* **2002**, *124*, 13688–13689.

5. Bachilo, S. M.; Balzano, L.; Herrera, J. E.; Pompeo, F.; Resasco, D. E.; Weisman, R. B. Narrow (*n*,*m*)-Distribution of Single-Walled Carbon Nanotubes Grown using a Solid Supported Catalyst. *J. Am. Chem. Soc.* **2003**, *125*, 11186–11187.

6. Nasibulin, A. G.; Pikhitsa, P. V.; Jiang, H.; Kauppinen, E. I. Correlation between Catalyst Particle and Single-Walled Carbon Nanotube Diameters. *Carbon* **2005**, *43*, 2251–2257.

7. Chiang, W.-H.; Sankaran, R. M. Linking Catalyst Composition to Chirality Distributions of As-Grown Single-Walled Carbon Nanotubes by Tuning Ni_xFe_{1-x} Nanoparticles. *Nat. Mater.* **2009**, *8*, 882–886.

8. Fiawoo, M.-F. C.; Bonnot, A.-M.; Amara, H.; Bichara, C.; Thibault-Pénisson, J.; Loiseau, A. Evidence of Correlation between Catalyst Particles and the Single-Wall Carbon Nanotube Diameter: A First Step Towards Chirality Control. *Phys. Rev. Lett.* **2012**, *108*, 195503.

9. Miyauchi, Y.; Chiashi, S.; Murakami, Y.; Hayashida, Y.; Maruyama, S. Fluorescence Spectroscopy of Single-Walled Carbon Nanotubes Synthesized from Alcohol. *Chem. Phys. Lett.* **2004**, *387*, 198–203.

10. Xiang, R.; Einarsson, E.; Murakami, Y.; Shiomi, J.; Chiashi, S.; Tang, Z.; Maruyama, S. Di-

ameter Modulation of Vertically Aligned Single-Walled Carbon Nanotubes. *ACS Nano* **2012**, *6*, 7472–7479.

11. Yao, Y.; Li, Q.; Zhang, J.; Liu, R.; Jiao, L.; Zhu, Y. T.; Liu, Z. Temperature-Mediated Growth of Single-Walled Carbon-Nanotube Intramolecular Junctions. *Nat. Mater.* **2007**, *6*, 283–286.

12. Zhu, W.; Rosen, A.; Bolton, K. Changes in Single-Walled Carbon Nanotube Chirality during Growth and Regrowth. *J. Chem. Phys.* **2008**, *128*, 124708.

13. Ning, G.; Shinohara, H. Unsynchronized Diameter Changes of Double-Wall Carbon Nanotubes during Chemical Vapour Deposition Growth. *Chem. Asian J.* **2009**, *4*, 955–960.

14. Hasegawa, K.; Noda, S. Moderating Carbon Supply and Suppressing Ostwald Ripening of Catalyst Particles to Produce 4.5-mm-Tall Single-Walled Carbon Nanotube Forests. *Carbon* **2011**, *49*, 4497–4504.

15. Murakami, Y.; Chiashi, S.; Miyauchi, Y.; Hu, M. H.; Ogura, M.; Okubo, T.; Maruyama, S. Growth of Vertically Aligned Single-Walled Carbon Nanotube Films on Quartz Substrates and their Optical Anisotropy. *Chem. Phys. Lett.* **2004**, *385*, 298–303.

16. Maruyama, S.; Einarsson, E.; Murakami, Y.; Edamura, T. Growth Process of Vertically Aligned Single-Walled Carbon Nanotubes. *Chem. Phys. Lett.* **2005**, *403*, 320–323.

17. Xiang, R.; Zhang, Z.; Ogura, K.; Okawa, J.; Einarsson, E.; Miyauchi, Y.; Shiomi, J.; Maruyama, S. Vertically Aligned ^{13}C Single-Walled Carbon Nanotubes Synthesized by No-Flow Alcohol Chemical Vapor Deposition and their Root Growth Mechanism. *Jpn. J. Appl. Phys.* **2008**, *47*, 1971–1974.

18. Thurakitseree, T.; Kramberger, C.; Zhao, P.; Aikawa, S.; Harish, S.; Chiashi, S.; Einarsson, E.; Maruyama, S. Diameter-Controlled and Nitrogen-Doped Vertically Aligned Single-Walled Carbon Nanotubes. *Carbon* **2012**, *50*, 2635–2640.

19. Thurakitseree, T.; Kramberger, C.; Zhao, P.; Chiashi, S.; Einarsson, E.; Maruyama, S. Reduction of Single-Walled Carbon Nanotube Diameter to Sub-nm via Feedstock. *Phys. Status Solidi B* **2012**, *in press*.

20. Kramberger, C.; Thurakitseree, T.; Koh, H.; Izumi, Y.; Kinoshita, T.; Muro, T.; Einarsson, E.; Maruyama, S. One-Dimensional N_2 Gas inside Single-Walled Carbon Nanotube Containers. *submitted*.

21. Einarsson, E.; Murakami, Y.; Kadowaki, M.; Maruyama, S. Growth Dynamics of Vertically Aligned Single-Walled Carbon Nanotubes from *in situ* Measurements. *Carbon* **2008**, *46*, 923–930.

22. Sumpter, B. G.; Meunier, V.; Romo-Herrera, J. M.; Cruz-Silva, E.; Cullen, D. A.; Terrones, H.; Smith, D. J.; Terrones, M. Nitrogen-Mediated Carbon Nanotube Growth: Diameter Reduction, Metallicity, Bundle Dispersability, and Bamboo-Like Structure Formation. *ACS Nano* **2007**, *1*, 369–375.

23. Kataura, H.; Kumazawa, Y.; Maniwa, Y.; Umezu, I.; Suzuki, S.; Ohtsuka, Y.; Achiba, Y. Optical Properties of Single-Wall Carbon Nanotubes. *Synth. Met.* **1999**, *103*, 2555–2558.

24. Dresselhaus, M. S.; Dresselhaus, G.; Saito, R.; Jorio, A. Raman Spectroscopy of Carbon Nanotubes. *Physics Reports* **2005**, *409*, 47–99.

25. Araujo, P. T.; Doorn, S. K.; Kilina, S.; Tretiak, S.; Einarsson, E.; Maruyama, S.; Chacham, H.; Pimenta, M. A.; Jorio, A. Third and Fourth Optical Transitions in Semiconducting Carbon Nanotubes. *Phys. Rev. Lett.* **2007**, *98*, 067401.

26. Koós, A. A.; Dillon, F.; Obraztsova, E. A.; Crossley, A.; Grobert, N. Comparison of Structural Changes in Nitrogen and Boron-Doped Multi-Walled Carbon Nanotubes. *Carbon* **2010**, *48*, 3033–3041.

27. Liu, H.; Zhang, Y.; Li, R.; Sun, X.; Désilets, S.; Abou-Rachid, H.; Jaidann, M.; Lussier, L.-S. Structural and Morphological Control of Aligned Nitrogen-Doped Carbon Nanotubes. *Carbon* **2010**, *48*, 1498–1507.

28. Pfeiffer, R.; Kuzmany, H.; Simon, F.; Bokova, S. N.; Obraztsova, E. Resonance Raman Scattering from Phonon Overtones in Double-Wall Carbon Nanotubes. *Phys. Rev. B* **2005**, *71*, 155409.

29. Cardenas, J. F.; Gromov, A. Double Resonance Raman Scattering in Solubilised Single Walled Carbon Nanotubes. *Chem. Phys. Lett.* **2007**, *442*, 409–412.

30. Chen, Y.; Ciuparu, D.; Lim, S.; Yang, Y.; Haller, G. L.; Pfefferle, L. Synthesis of Uniform Diameter Single Wall Carbon Nanotubes in Co-MCM-41: Effects of CO Pressure and Reaction Time. *J. Catal.* **2004**, *226*, 351–362.

31. Picher, M.; Anglaret, E.; Arenal, R.; Jourdain, V. Processes Controlling the Diameter Distribution of Single-Walled Carbon Nanotubes during Catalytic Chemical Vapor Deposition. *ACS Nano* **2011**, *5*, 2118–2125.

32. Wei, D. C.; Liu, Y. Q.; Cao, L. C.; Fu, L.; Li, X. L.; Wang, Y.; Yu, G.; Zhu, D. B. A New Method to Synthesize Complicated Multibranched Carbon Nanotubes with Controlled Architecture and Composition. *Nano Lett.* **2006**, *6*, 186–192.

33. Ouyang, M.; Huang, J. L.; Lieber, C. M. Fundamental Electronic Properties and Applications of Single-Walled Carbon Nanotubes. *Acc. Chem. Res.* **2002**, *35*, 1018–1025.

34. Jin, Z.; Li, X.; Zhou, W.; Han, Z.; Zhang, Y.; Li, Y. Direct Growth of Carbon Nanotube Junctions by a Two-Step Chemical Vapor Deposition. *Chem. Phys. Lett.* **2006**, *432*, 177–183.

35. Li, J.; Papadopoulos, C.; Xu, J. Nanoelectronics: Growing Y-Junction Carbon Nanotubes. *Nature* **1999**, *402*, 253–254.

36. Meng, G. W.; Jung, Y. J.; Cao, A. Y.; Vajtai, R.; Ajayan, P. M. Controlled Fabrication of Hierarchically Branched Nanopores, Nanotubes, and Nanowires. *Proc. Natl. Acad. Sci. U. S. A.* **2005**, *102*, 7074–7078.

37. Wei, D.; Cao, L.; Fu, L.; Li, X.; Wang, Y.; Yu, G.; Liu, Y. A New Technique for Controllably Producing Branched or Encapsulating Nanostructures in a Vapor-Liquid-Solid Process. *Adv. Mater.* **2007**, *19*, 386–390.

38. Ouyang, M.; Huang, J. L.; Cheung, C. L.; Lieber, C. M. Atomically Resolved Single-Walled Carbon Nanotube Intramolecular Junctions. *Science* **2001**, *291*, 97–100.

39. Chico, L.; Crespi, V. H.; Benedict, L. X.; Louie, S. G.; Cohen, M. L. Pure Carbon Nanoscale Devices: Nanotube Heterojunctions. *Phys. Rev. Lett.* **1996**, *76*, 971–974.

40. Ayala, P.; Arenal, R.; Rümmeli, M.; Rubio, A.; Pichler, T. The Doping of Carbon Nanotubes with Nitrogen and their Potential Applications. *Carbon* **2010**, *48*, 575–586.

41. O'Byrne, J. P.; Li, Z.; Jones, S. L. T.; Fleming, P. G.; Larsson, J. A.; Morris, M. A.; Holmes, J. D. Nitrogen-Doped Carbon Nanotubes: Growth, Mechanism and Structure. *ChemPhysChem* **2011**, *12*, 2995–3001.

42. Hafner, J. H.; Bronikowski, M. J.; Azamian, B. R.; Nikolaev, P.; Rinzler, A. G.; Colbert, D. T.; Smith, K. A.; Smalley, R. E. Catalytic Growth of Single-Wall Carbon Nanotubes from Metal Particles. *Chem. Phys. Lett.* **1998**, *296*, 195–202.

43. Zhang, Z.; Einarsson, E.; Murakami, Y.; Miyauchi, Y.; Maruyama, S. Polarization dependence of radial breathing mode peaks in resonant Raman spectra of vertically aligned single-walled carbon nanotubes. *Physical Review B* **2010**, *81*, 165442.

Graphical TOC Entry

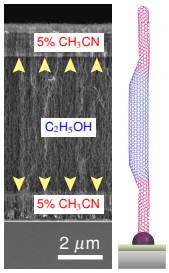

Changing the carbon feedstock from pure ethanol to a 5 vol.% mixture of acetonitrile in ethanol during growth of vertically aligned SWNTs changes the mean diameter of the emerging layer significantly from 2 to less than 1 nm. The change is reversible, as demonstrated by triple layer sandwich structures. Controlling the mean diameter along growing nanotubes opens up new possibilities for bottom up production nano-carbon based devices.